Chapter 5
Parameter Uncertainties

This chapter uses an *incremental* bond graph approach in order to determine parameter sensitivities of ARR residuals as well as adaptive mode-dependent ARR thresholds for systems described by a hybrid model. To that end, first, the underlying idea and some basics of incremental bond graphs are briefly recalled.

5.1 Introduction

In order to avoid that false alarms are reported to a supervisor system or that true faults are not detected, ARR residuals should be significantly sensitive to true faults but little sensitive to parameter variations given uncertain system parameter values. Parameter sensitivities of ARR residuals can be singled out by defining appropriate thresholds. As the dynamic behaviour of a real system described by a hybrid model can be quite different in different system modes, thresholds should be adapted to system modes.

If ARRs can be obtained in closed symbolic form, parameter sensitivities can be determined by symbolic differentiation with respect to parameters. If this is not possible, parameter sensitivities of ARRs can be computed numerically by using either a *sensitivity* bond graph [1–4] or an *incremental* bond graph [5, 6]. Incremental bond graphs were initially introduced for the purpose of frequency domain sensitivity analysis of LTI models. Furthermore, they have also proven useful for the determination of parameter sensitivities of state variables and output variables, transfer functions of the direct model as well as of the inverse model, and for the determination of ARR residuals from continuous time models [7, Chap. 4]. In this chapter, the incremental bond graph approach is applied to systems described by switched LTI systems.

As to FDI robust with regard to parameter uncertainties, an approach based on so-called uncertain bond graphs in linear fractional transformation form (LFT) has been reported in the literature [8–10] for time-continuous models. In an uncertain bond graph, bonds carry power variables uncertain with regard to parameter variations

W. Borutzky, *Bond Graph Model-based Fault Diagnosis of Hybrid Systems*,
DOI 10.1007/978-3-319-11860-4_5

and bond graph elements are decomposed into a part with nominal parameters and another one with uncertain parameters.

In contrast, in an incremental bond graph, bonds carry variations of power variables, and variations of ARR residuals are outputs of special interest. In the case of switched LTI systems with uncertain parameters, variations of ARR residuals are a weighted sum of variations of power variables. The weighting factors depend on power variables of the original bond graph. The weighted sum suggests to apply the triangle inequality to obtain adaptive bounds for the part of an ARR residual that is uncertain due to parameter variations. The nominal part of an ARR residual is obtained from the original bond graph with nominal parameters.

An incremental bond graph can be constructed in a systematic manner from the original bond graph of a switched LTI system by replacing an element that is due to parameter variations by its incremental element model. Equations for variations of power variables can be automatically derived in the same way as they are derived from an initial bond graph with nominal parameters.

5.2 Incremental Bond Graphs for Switched LTI Systems

Switched LTI systems are just LTI systems for the time intervals betweens between discrete mode changes. Therefore, first, the incremental bond graph approach is recalled for LTI systems. In a second step, an incremental model for switches is proposed.

5.2.1 Incremental Models of Bond Graph Elements

In order to simplify the presentation, it is assumed that energy sources, energy storage elements and resistors are linear 1-port elements and that transformers and gyrators have got two ports.

The underlying idea of incremental bond graphs is that if a parameter Θ of a component model varies, then both power variables at its port are perturbed due to its interaction with the ports of other elements in the model. That is, an effort $e_n(t)$ in a bond graph with nominal parameters becomes $e(t) = e_n(t) + \Delta e(t)$. The same holds for the conjugate power variable $f(t)$. In incremental bond graphs, bonds carry the increments $\Delta e(t)$, $\Delta f(t)$ of power variables. In other words, they represent energy flows carrying the amount of power $\Delta e(t) \cdot \Delta f(t)$.

An incremental bond graph of an LTI system is constructed from an initial bond graph with nominal parameters by replacing those bond graph elements by their incremental model for which a parameter variation has taken place. Clearly, sources that do not depend on a parameter become null sources. Furthermore, the incremental model of a 1(0)-junction remains a 1(0)-junction. As to the incremental models of storage elements, resistors, transformers and gyrators, it turns out that they differ from the respective element just by modulated sinks added to junctions. The sinks

are modulated by a power variable of the initial bond graph. That is, the structure of the initial bond graph is retained by the incremental bond graph. Structurally, both bond graphs only differ with respect to sources and sinks and their location. As a result, existing software can be used to set up a state space model for the variations of the state variables.

In order to see how an incremental bond graph model for a bond graph element is obtained, a linear 1-port C-element with the nominal capacitance C_n is considered. In the following, an index n indicates a parameter or a variable of the non-faulty bond graph model with nominal parameters. In the case of a time constant parameter variation ΔC the linear constitutive equation of a 1-port C element in derivative causality takes the form

$$f_C(t) = f_{C_n}(t) + (\Delta f_C)(t) = (C_n + \Delta C)(\dot{e}_{C_n} + (\Delta \dot{e}_C))(t) \tag{5.1}$$

Expanding the right hand side yields

$$\begin{aligned}(\Delta f_C)(t) &= C_n(\Delta \dot{e}_C)(t) + (\Delta C)\dot{e}_C(t) \\ &= C_n(\Delta \dot{e}_C)(t) + \underbrace{\frac{\Delta C}{C}}_{=:\,\delta_C} f_C(t)\end{aligned} \tag{5.2}$$

Figure 5.1 shows a bond graph representation of (5.2). In essence, the incremental model of a C element is again a C element. A modulated sink MSe : $\delta_C f_C$ contributes to its output Δf_C.

The power variable f_C controlling the modulated source is an output variable of the original bond graph model. If f_C has been obtained by measurements of the real system, then the contribution to the output of the incremental bond graph model of the C element may contain sensor noise. In any case, the outputs of the incremental bond graph of a bond graph element indicate a parameter variation.

Recall that in FDI, energy storage elements are in preferred derivative causality because initial conditions are not known or difficult to obtain in real time FDI. In offline simulation, the storage elements in the non-faulty model may be in preferred integral causality. Reformulation of (5.2) gives

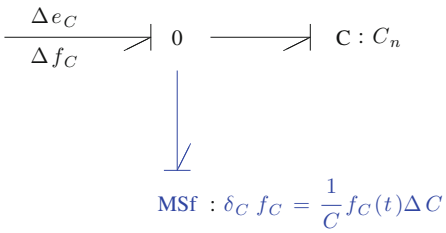

Fig. 5.1 Incremental bond graph model of a linear 1-port C element in preferred derivative causality

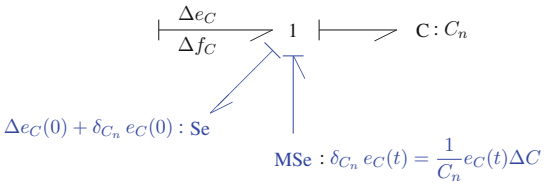

Fig. 5.2 Incremental bond graph model of a linear 1-port C element in preferred integral causality

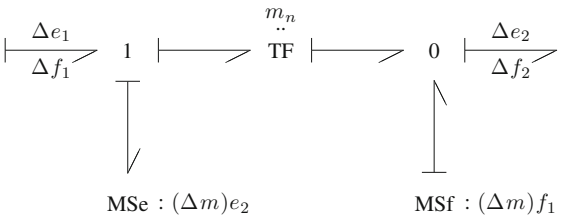

Fig. 5.3 Incremental bond graph model of a 2-port transformer

$$\Delta e_C(t) = \frac{1}{C_n} \int_0^t (\Delta f)(\tau) d\tau - \delta_{C_n}(e_C(t) - e_c(0)) + \Delta e_C(0) \tag{5.3}$$

where $\delta_{C_n} := \Delta C / C_n$. Equation 5.3 may be represented by the bond graph model in Fig. 5.2.

In the same manner, incremental models for the other bond graph elements may be obtained. As an example, Fig. 5.3 depicts the incremental bond graph model of a transformer TF : m_n.

5.2.2 *Incremental Models of Nonlinear Bond Graph Elements*

The incremental bond graph approach is not limited to linear 1-port elements with one parameter [5]. The constitutive equation of the incremental model of a bond graph element can be easily obtained by taking the total differential of the constitutive equation of the bond graph element.

For instance, let

$$q(t) = \Phi(e(t), \theta) \tag{5.4}$$

be the constitutive equation of a nonlinear 1-port C element, $\theta = \Theta_n + \Delta\Theta$ its parameter and $\Delta\Theta$ a time constant deviation from the nominal value Θ_n. Then

$$f(t) = \dot{q}(t) = \frac{\partial \Phi(e(t), \theta)}{\partial e} \cdot \dot{e}(t) = f(e(t), \dot{e}(t), \theta) \tag{5.5}$$

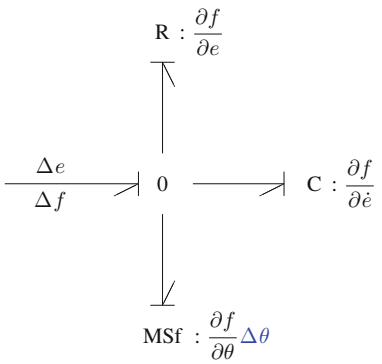

Fig. 5.4 Incremental bond graph model of a nonlinear 1-port C element in preferred derivative causality

and

$$\Delta f = \frac{\partial f}{\partial e}\Delta e + \frac{\partial f}{\partial \dot{e}}\Delta \dot{e} + \frac{\partial f}{\partial \theta}\Delta\theta \tag{5.6}$$

Equation 5.6 may be represented by an incremental bond graph model with nonlinear elements as depicted in Fig. 5.4.
In Fig. 5.4, the partial derivatives of f may be complex expressions depending on the nonlinear function Φ.

5.2.3 An Incremental Model of the Non-ideal Switch

For the sake of a unified bond graph representation of hybrid models that hold for all system modes, in this book, non-ideal switches are used and are represented by means of an MFT : $m_{\mathrm{sw}}(t)$ with $m_{\mathrm{sw}}(t) \in \{0, 1\}\ \forall\ t \geq 0$ in conjunction with a resistor R : R_{on} in fixed conductance causality (Fig. 2.12b).

In ON-mode, the switch model simply reduces to a resistor with the small nominal ON-resistance R^n_{on}. The constitutive equation of a linear 1-port resistor in conductance causality then leads to an equation for the increments of the power variables.

$$f_{\mathrm{sw}}(t) \;=\; f^n_{\mathrm{sw}}(t) + (\Delta f_{\mathrm{sw}})(t) = \frac{1}{R^n_{\mathrm{on}} + \Delta R_{\mathrm{on}}}\left(e^n_{\mathrm{sw}}(t) + \Delta e_{\mathrm{sw}}(t)\right) \tag{5.7}$$

Reformulation yields

$$(\Delta f_{\mathrm{sw}})(t) = \frac{1}{R^n_{\mathrm{on}}}(\Delta e_{\mathrm{sw}})(t) - \underbrace{\frac{\Delta R_{\mathrm{on}}}{\mathrm{R}^n_{\mathrm{on}}}}_{=:\,\delta_{R_{\mathrm{on}}}} f_{\mathrm{sw}}(t) \tag{5.8}$$

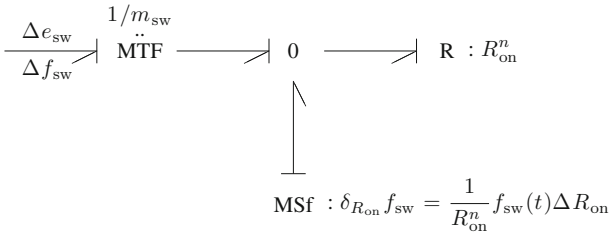

Fig. 5.5 Incremental bond graph model of a non-ideal switch

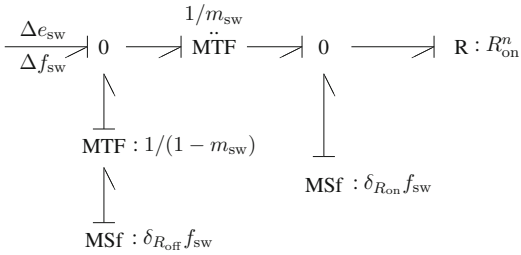

Fig. 5.6 Extended incremental bond graph model of a non-ideal switch accounting for a non-zero flow in OFF-mode

In OFF-mode, $f_{\rm sw} = 0$. Hence, $\Delta f_{\rm sw} = 0$. Figure 5.5 depicts an incremental bond graph model of a non-ideal switch that captures both switch states.

If the flow close to zero in OFF-mode is not neglected, then the switch in OFF-mode can be considered a resistor with a very high OFF resistance $\rm R_{off}$. For this resistor, an incremental model can be developed in the same manner as for the resistor $\rm R : \mathit{R}_{on}$. In the resulting model, the resistor $\rm R : \mathit{R}_{off}$ can be neglected as the nominal value of $1/R_{\rm off}$ is very small. Figure 5.6 depicts an extended incremental bond graph model of a non-ideal switch that accounts for a non-zero flow in OFF-mode.

The incremental bond graph model of a linear 1-port resistor $\rm R : \mathit{R}_n$ in resistance causality is obtained by solving (5.8) for Δe.

$$\Delta e_R(t) = R_n \Delta f_R(t) + R_n \delta_{R_n} f_R(t) \tag{5.9}$$

in accordance with Fig. 5.7.

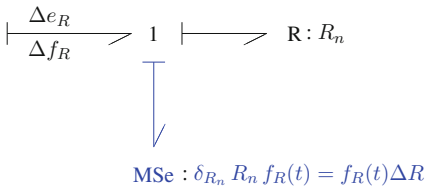

Fig. 5.7 Incremental bond graph model of a linear 1-port resistor in resistance causality

5.3 Incremental Bond Graphs for FDI

Given incremental models for all bond graph elements, an incremental bond graph (incBG) can be systematically constructed from a bond graph of the non-faulty system with nominal parameters by replacing sources of constant value by sources of value zero and by replacing elements with varying parameters by their incremental bond graph model. As the incremental model of a bond graph element differs from the element only by modulated sinks representing parameter variations, the incremental bond graph retains the structure of the original bond graph. The incremental DBG differs from the initial DBG only with respect to the sources and the additional sinks modulated by a power variable of the original BG. The number of these additional sinks equals the number of varying parameters. If the original model is given by a switched LTI system so is the incremental bond graph model. Hence, the incremental model and the original one have the same system matrix $\mathbf{A}$ with nominal parameters. Existing software can be used to derive equations from the incremental DBG and to set up the matrices of a switched LTI system in symbolic form in the same manner as for the original DBG.

Let $\boldsymbol{u}$ denote the vector of inputs into the original bond graph model with nominal parameters, $\boldsymbol{x}$ its state vector composed of all inputs into storage elements in preferred derivative causality and let an index n indicate a dependency from nominal parameter values. The state space model derived from the original bond graph then reads

$$\dot{\boldsymbol{x}}(t) = \mathbf{A}_n \boldsymbol{x}(t) + \mathbf{B}_n \boldsymbol{u}(t), \quad \boldsymbol{x}(0) = \boldsymbol{x}_0 \tag{5.10a}$$

$$\boldsymbol{y}(t) = \mathbf{C}_n \boldsymbol{x}(t) \tag{5.10b}$$

Furthermore, let $\boldsymbol{\Theta}$ denote the vector of all component parameters. The state space model derived from the incremental bond graph then is of the form

$$\Delta\dot{\boldsymbol{x}}(t) = \mathbf{A}_n \Delta\boldsymbol{x}(t) + \mathbf{B}^*(\boldsymbol{\Theta}_n)\boldsymbol{w}(t) \tag{5.11a}$$

$$\Delta\boldsymbol{y}(t) = \mathbf{C}_n \Delta\boldsymbol{x}(t) \tag{5.11b}$$

The matrices $\mathbf{A}_n$ and $\mathbf{C}_n$ are obtained deriving equations from the original bond graph with nominal parameters. Matrix $\mathbf{B}^*$ can be automatically set up from the incremental bond graph. The vector $\boldsymbol{w}$ denotes the outputs of the modulated sinks in the incremental bond graph that represent parameter variations. These outputs are of the form

$$\boldsymbol{w}(t) = \mathrm{diag}(\delta_i z_i(t))\Delta\boldsymbol{\Theta} \tag{5.12}$$

where diag() is a diagonal matrix and z_i a power variable from the original bond graph controlling the ith modulated sink that represents a parameter variation. The coefficients δ_i depend on the type of the bond graph element that has been replaced by its incremental model. For a capacitor for instance, $\delta_i = 1/C^i$ and $z_i = f_C^i$

(cf. Fig. 5.1). For a linear resistor in conductance causality with nominal resistance R_n, $\delta_i = 1/R_n$ and $z_i = f_R^i$ (cf. Fig. 5.5).

5.3.1 Parameter Sensitivities of ARR Residuals

Inputs to an incremental bond graph are the outputs of the sinks representing a parameter variation. They are modulated by a power variable from the original bond graph. Outputs of the incremental bond graph model with respect to FDI are variations Δr_i of ARR residuals r_i. In the case of a switched LTI system, they can be expressed as a weighted sum of the inputs and their time derivatives into the incremental bond graph. As the weighting factors may include transformer moduli $m_i(t) \in \{0, 1\}$, variations of ARR residuals are system mode dependent. According to (5.11a, 5.11b) and (5.12), there is a matrix $\mathbf{C}_n$ such that the Laplace transform of the variation of the ith residual r_i reads

$$\mathscr{L}\Delta r_i = \sum_{j=1}^{m} F_{ij}^* \underbrace{\delta_j \, (\mathscr{L} z_j) \, \Delta\Theta_j}_{\mathscr{L} w_j} \tag{5.13}$$

where

$$(F_{ij}^*) = \mathbf{C}_n (s\mathbf{I} - \mathbf{A}_n)^{-1} \mathbf{B}^* \tag{5.14}$$

Hence, the parameter sensitivity of ARR residual r_i with respect to the jth parameter Θ_j is

$$\mathscr{L} \frac{\partial r_i}{\partial \Theta_j} = F_{ij}^* \delta_j \mathscr{L} z_j \tag{5.15}$$

The power variable z_j is an output variable of the original bond graph model with nominal parameters and as such it is a weighted sum of the inputs $u_k(t)$ into the original bond graph in the case of a switched LTI system.

$$\mathscr{L} z_j = \sum_{k=1}^{n} F_{jk} \mathscr{L} u_k \tag{5.16}$$

where

$$(F_{jk}) = \mathbf{C}(s\mathbf{I} - \mathbf{A})^{-1} \mathbf{B} \tag{5.17}$$

As a result, parameter sensitivities of ARR residuals r_i with respect to parameter Θ_j can be obtained by constructing a matrix $\mathbf{F}$ from the matrices of the original

bond graph and a matrix $\mathbf{F}^*$ from the matrices of the incremental bond graph and by multiplying the ith row of matrix $\mathbf{F}$ by the factor $F^*_{ij}\delta_j$.

$$\mathscr{L}\frac{\partial r_i}{\partial \Theta_j} = F^*_{ij}\delta_j \sum_{k=1}^{n} F_{jk}\,\mathscr{L}u_k \tag{5.18}$$

These operations can be hardly manually performed, even for models of small size. However, a bond graph preprocessor such as CAMPG [11] can automatically derive the equations from the original as well as from the incremental bond graph. MATLAB®[12] or Scilab [13] script files can then generate the matrices $\mathbf{F}$ and $\mathbf{F}^*$ in symbolic form and can perform the multiplication of a row of $\mathbf{F}$ by the factor $F^*_{ij}\delta_j$ for each requested parameter sensitivity of an ARR residual.

For small switched LTI systems, variations of ARR residuals can be manually derived from an incremental bond graph by applying the principle of superposition. That is, only one bond graph element at a time is assumed to have an uncertain parameter. It is replaced by its incremental model. Detectors are replaced by a dual virtual detector for the variation of an ARR residual. Summing variations of flows or efforts, respectively, at these junctions and eliminating unknowns yields variations of residuals of ARRs as a weighted sum of the inputs supplied by those modulated sinks that represent parameter variations. The weighting factors in these sums are the sensitivities to be determined.

Example: Network with a Semiconductor Switch

As an example, the circuit with one switch in Fig. 4.1, is considered. To keep the illustration of the procedure short and simple it is assumed that only one parameter is uncertain. Accordingly, the incremental bond graph is obtained by replacing the element by its incremental model and by replacing the constant voltage source Se : V_i by an effort source of value zero and by replacing detectors by dual virtual detectors for the variations of ARR residuals.

Parameter R_1 Is Uncertain

Figure 5.8 displays the corresponding incremental bond graph. Again, the purpose of the auxiliary storage element C : C_a is just to resolve the causal conflict at junction 0_2. In the process of equation formulation, the capacitance C_a is set to zero. Summing variations of power variables at junctions 1_1, 0_2, and i_3 yields

$$1_1: \quad \Delta\tilde{r}_1 = 0 - f\,\Delta R_1 - \Delta u \tag{5.19a}$$

$$0_2: \quad 0 = C_1^n \Delta\dot{u}_{C_1} + \underbrace{C_a}_{\approx 0}\Delta\dot{u} + \Delta i_{\mathrm{sw}} \tag{5.19b}$$

$$1_3: \quad \Delta i_{\mathrm{sw}} = \frac{b}{R^n_{\mathrm{on}}}(\Delta u_{C_1} - R_2^n \Delta i_{\mathrm{sw}} - 0) \tag{5.19c}$$

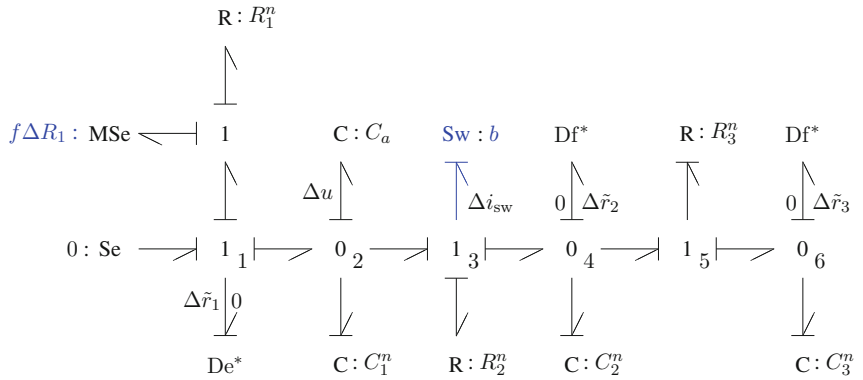

Fig. 5.8 Incremental bond graph of the switched circuit in Fig. 4.1 in the case of an uncertain parameter R_1

Combining (5.19a)–(5.19c) gives

$$\Delta r_1 := -C_1^n \Delta\dot{\tilde{r}}_1 - \frac{b}{R_{\mathrm{on}}^n + R_2^n}\Delta\tilde{r}_1 = C_1^n \dot{f}\,\Delta R_1 + \frac{b}{R_{\mathrm{on}}^n + R_2^n} f\,\Delta R_1 \quad (5.20)$$

Hence,

$$\frac{\partial r_1}{\partial R_1} = C_1^n \dot{f} + \frac{b}{R_{\mathrm{on}}^n + R_2^n} f \quad (5.21)$$

in accordance with (4.6).

Sensitivity $\partial r_2/\partial R_1$ is likewise obtained. Summation of flow variations at junction 0_4 yields

$$\Delta\tilde{r}_2 = \Delta i_{\mathrm{sw}} \quad (5.22)$$

Reformulation gives

$$\Delta r_2 := \Delta\tilde{r}_2 + \frac{b}{R_{\mathrm{on}}^n + R_2^n}\Delta\tilde{r}_1 = -\frac{b}{R_{\mathrm{on}}^n + R_2^n} f\,\Delta R_1 \quad (5.23)$$

Thus,

$$\frac{\partial r_2}{\partial R_1} = -\frac{b}{R_{\mathrm{on}}^n + R_2^n} f \quad (5.24)$$

in accordance with (4.7).

Parameter R_3 Is Uncertain

Figure 5.9 displays the corresponding incremental bond graph. Summation of flow variations at junction 0_6 gives

$$\Delta r_3 = -\frac{1}{R_3^n}\, i_3\, \Delta R_3 \;=\; -\frac{1}{R_3^n}\, C_3^n\, \dot{e}_2\, \Delta R_3 \tag{5.25}$$

and

$$\Delta r_3 := R_3^n \Delta \tilde{r}_3 \;=\; -\, C_3^n\, \dot{e}_2\, \Delta R_3 \tag{5.26}$$

Thus

$$\frac{\partial r_3}{\partial R_3} = -\, C_3^n\, \dot{e}_2 \tag{5.27}$$

in accordance with (4.8).
Likewise,

$$\Delta r_2 := \Delta \tilde{r_2} \;=\; \Delta i_{\mathrm{sw}} + \frac{1}{R_3^n}\, i_3\, \Delta R_3 \;=\; \Delta i_{\mathrm{sw}} + \frac{e_1 - e_2}{(R_3^n)^2}\, \Delta R_3 \tag{5.28}$$

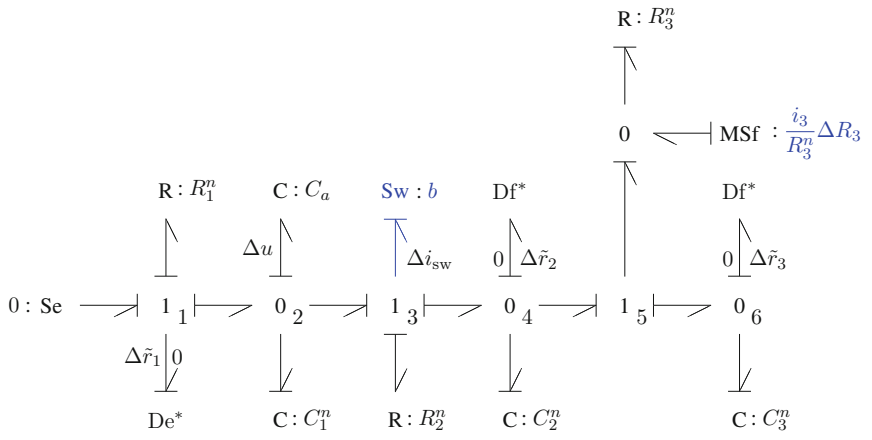

Fig. 5.9 Incremental bond graph of the switched circuit in Fig. 4.1 in the case of an uncertain parameter R_3

and

$$\frac{\partial r_2}{\partial R_3} = \frac{1}{(R_3^n)^2}\,(e_1 - e_2) \tag{5.29}$$

in accordance with (4.7).

5.3.2 *Adaptive Mode-Dependent Thresholds for Parameter Variations of ARR Residuals*

According to (5.13), the Laplace transform of the variation of an ARR residual is a weighted sum of the inputs into the incremental bond graph. The weighting factors are transfer functions

$$F_{ij}^*(s) = \frac{N_{ij}^*(s)}{D^*(s)} \tag{5.30}$$

where $N_{ij}^*(s)$ and $D^*(s)$ are polynomials and $s \in \mathbb{C}$.

Let $(n_{ij}^*)_\kappa$ be the κth coefficient of the polynomial $N_{ij}^*(s)$ and $\delta_{\Theta_j} := \delta_j \Delta\Theta_j$. Then

$$\begin{aligned} \mathscr{L}\Delta r_i := D^* \mathscr{L}\Delta\tilde{r}_i &= \sum_j \delta_{\Theta_j} N_{ij}^*(s) \mathscr{L} z_j \\ &= \sum_j \delta_{\Theta_j} \sum_{\kappa=0}^{k_j} (n_{ij}^*)_\kappa\, s^\kappa \mathscr{L} z_j \end{aligned} \tag{5.31}$$

or in the time domain

$$\Delta r_i(t) = \sum_j \delta_{\Theta_j} \sum_{\kappa=0}^{k_j} (n_{ij}^*)_\kappa\, z_j^{(\kappa)} \tag{5.32}$$

The sum in (5.32) suggests in a natural way to apply the triangle inequality in order to define an adaptive upper bound for the absolut values of parameter variations of ARR residuals.

$$|\Delta r_i(t)| \le \sum_j \sum_k |\delta_{\Theta_j} (n_{ij}^*)_k\, z_j^{(k)}| =: thr_i(t) \tag{5.33}$$

No fault is reported as along as variations of ARR residuals due to uncertain parameters are within the adaptive bounds $\pm\, thr_i(t)$.

As a result, ARR residuals as fault indicators may be obtained by evaluating ARRs derived from a diagnostic bond graph with nominal parameters. In order to assess the effect of uncertain parameters on ARR residuals, parameter variations of ARR residuals may be derived from an incremental bond graph. Application of the triangle inequality then gives adaptive bounds for these variations.

Example: Simple Network with a Semiconductor Switch

This way of determining adaptive thresholds for parameter variations of ARR residuals is illustrated by means of the network displayed in Fig. 5.10 which is a simplification of the switched circuit in Fig. 4.1.

Figure 5.11 shows a diagnostic bond graph of the simple switched RC-circuit. For this circuit, ARRs (4.6)–(4.7) simplify to

$$0_2: \qquad r_1 = 0 = f - C_1(\dot{V}_i - R_1\dot{f}) - \frac{b}{R_{\text{on}} + R_2}(V_i - R_1 f - e_1) \tag{5.34a}$$

$$0_4: \qquad r_2 = 0 = \frac{b}{R_{\text{on}} + R_2}(V_i - R_1 f - e_1) - C_2\dot{e}_1 \tag{5.34b}$$

Figure 5.12 displays the corresponding incremental bond graph.

It is assumed that the small ON-resistance of the switch and resistance R_2 are not uncertain. Therefore, the switch model Sw : b and resistor R : R_2 haven't been

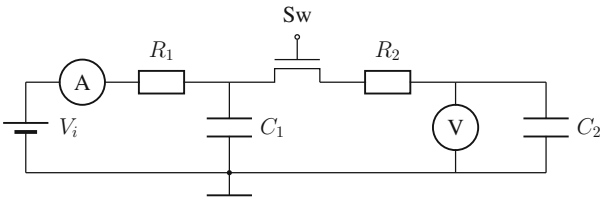

Fig. 5.10 Simple RC-circuit with a semiconductor switch

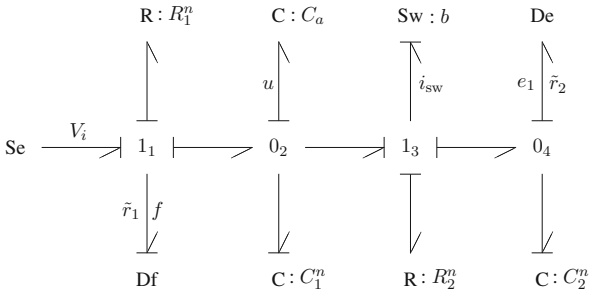

Fig. 5.11 Diagnostic bond graph of the simple switched RC-circuit

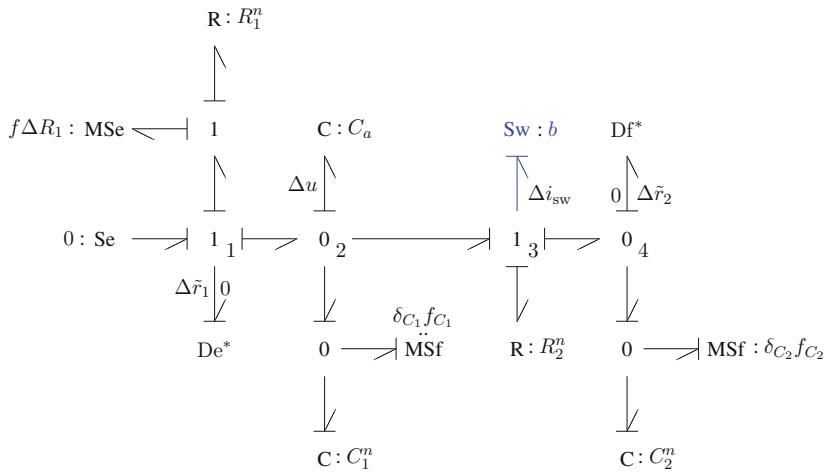

Fig. 5.12 Incremental bond graph of the simple circuit in Fig. 5.10

replaced by their incremental model. Summation of variations of power variables at the junctions yields

$$1_1: \quad \Delta\tilde{r}_1 = 0 - f\,\Delta R_1 - \Delta u \tag{5.35a}$$

$$0_2: \quad 0 = C_1^n \Delta\dot{u} + \delta_{C_1} f_{C_1} + \underbrace{C_a}_{\approx 0} \Delta\dot{u} + \Delta i_{sw} \tag{5.35b}$$

$$1_3: \quad \Delta i_{sw} = \frac{b}{R_{on}^n}(\Delta u - 0 - R_2^n\,\Delta i_{sw}) \tag{5.35c}$$

$$0_4: \quad \Delta\tilde{r}_2 = \Delta i_{sw} - \delta_{C_2} f_{C_2} \tag{5.35d}$$

Combination of (5.35a)–(5.35d) gives for variations of the residuals Δr_1, Δr_2:

$$\begin{aligned}\Delta r_1 &:= -C_1^n \Delta\ddot{\tilde{r}}_1 - \frac{b}{R_{on}^n + R_2^n}\Delta\dot{\tilde{r}}_1 \;=\; C_1^n \ddot{f}\,\Delta R_1 - \delta_{C_1}\dot{f}_{C_1} + \frac{b}{R_{on}^n + R_2^n} f\,\Delta R_1 \\ &= \delta_{R_1} R_1^n C_1^n \ddot{f} - \delta_{C_1} \underbrace{C_1(\ddot{V}_i - R_1\ddot{f})}_{\dot{f}_{C_1}} + \frac{b}{R_{on}^n + R_2^n}\delta_{R_1} R_1^n \dot{f}\end{aligned} \tag{5.36a}$$

$$\begin{aligned}\Delta r_2 &:= \Delta\dot{\tilde{r}}_2 + \frac{b}{R_{on}^n + R_2^n}\Delta\tilde{r}_1 \;=\; -\frac{b}{R_{on}^n + R_2^n} f\,\Delta R_1 - \delta_{C_2}\dot{f}_{C_2} \\ &= -\frac{b}{R_{on}^n + R_2^n}\delta_{R_1} R_1 \dot{f} - \delta_{C_2} C_2 \ddot{e}_1\end{aligned} \tag{5.36b}$$

Adaptive mode dependent thresholds thr_1, thr_2 for parameter variations of ARR residual thus can be chosen as

$$|\Delta r_1| \leq |\delta_{R_1} R_1^n C_1^n \dot{f}| + |(\Delta C_1)(\dot{V}_i - R_1 \dot{f})| + |\frac{b}{R_{\text{on}}^n + R_2^n} \delta_{R_1} R_1 f| =: thr_1(t) \tag{5.37a}$$

$$|\Delta r_2| \leq |\frac{b}{R_{\text{on}}^n + R_2^n} \delta_{R_1} R_1^n f| + |(\Delta C_2)\dot{e}_1| =: thr_2(t) \tag{5.37b}$$

Remark 5.1 The same results for Δr_1 and Δr_2 are obtained by taking the total differential of ARRs (5.34a)–(5.34b). □

Fault Scenario: The Value of Capacitance C_1 Is Changed for Some Time Interval

The simulated fault scenario assumes that capacitance $C_1(t)$ is reduced to 20 % of its initial nominal value C_1^n for 2 s $< t <$ 4 s and is restored to C_1^n for $t >$ 4 s.

$$C_1(t) = C_1^n - dC_1 \cdot \texttt{pulse(t,2,4)} \tag{5.38}$$

where $dC_1 = 80/100 \cdot C_1^n$ and `pulse(t,2,4)` denotes a unit pulse lasting from 2 to 4 s.

According to (5.34a)–(5.34b), residual r_1 is sensitive to a change in capacitance C_1 independent of the two system modes determined by the switch state b, while residual r_2 is insensitive of C_1 in both modes. To show this mode independence, the closed switch is opened at $t = 3.5$ s. That is, a mode change happens while parameter C_1 has a significantly reduced value. For the determination of adaptive threshold bounds a constant relative parameter variation of 2 % has been adopted for parameters R_1, R_2, C_1 and C_2. Table 5.1 lists the parameter used by the simulation of the fault scenario.

First, Fig. 5.13a, b indicate the time evolutions of the capacitor voltages u_{C_1}, $\tilde{u}_{C_1}$, u_{C_2}, $\tilde{u}_{C_2}$ and of the currents $\tilde{i}_{R_1}$ and $\tilde{i}_{C_1}$ respectively as would be expected. The tilde and the prefixing letter 't' in the figures denote variables of the perturbed

Table 5.1 Parameters used by the simulation of the fault scenario

Parameter	Value	Units
E	5	V
R_1^n	100	kΩ
C_1^n	10	μF
dC_1	8 (2s $< t <$ 4s)	μF
C_2^n	10	μF
δ_{R_1}	2 %	–
δ_{R_2}	2 %	–
δ_{C_1}	2 %	–
δ_{C_2}	2 %	–

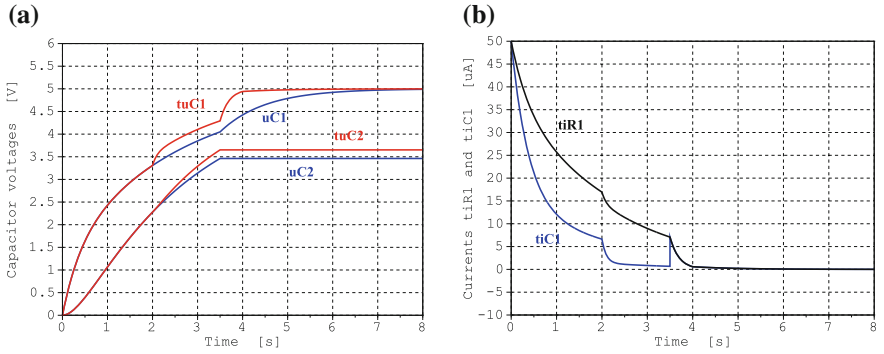

Fig. 5.13 Time evolution of the capacitor voltages and of currents $\tilde{i}_{R_1}$ and $\tilde{i}_{C_1}$. **a** Time history of capacitor voltages. **b** Time history of currents $\tilde{i}_{R_1}$ and $\tilde{i}_{C_1}$

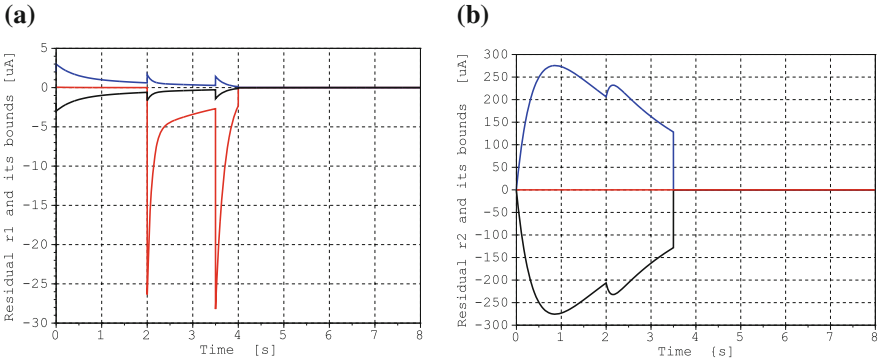

Fig. 5.14 Residuals r_1, r_2 and their adaptive thresholds. **a** Time evolution of residual r_1 and its adaptive thresholds $\pm\, thr_1$ **b** Time evolution of residual r_1 and its thresholds $\pm\, thr_2$

system. Both figures clearly show the effect of the reduction of capacitance C_1 for the time interval [2 s, 4 s] and the effect of the opening the switch at $t = 3.5$ s.

Figure 5.14a, b display the time evolution of residual r_1, r_2 and their adaptive thresholds $\pm\, thr_1, \pm\, thr_2$.

Figure 5.14b confirms that residual r_2 is insensitive to a change in capacitance C_1 independent of the system mode. The time history of residual r_1 in Fig. 5.14a shows a spike at $t = 2$ s due to the abrupt decrease of capacitance C_1 and another spike at $t = 3.5$ s due to the opening of the switch. Moreover, for the time interval [2 s, 4 s] in which C_2 is significantly reduced, values of r_1 are clearly below the adaptive lower bound $-thr_1$ indicating a fault. Outside of this time interval, the values of r_1 are well inside the narrow adaptive bounds. That is, r_1 is sensitive in both system modes to the temporary parametric fault in C_1 but insensitive to a 2 % relative parameter variation of parameters R_1, R_2, C_1 and C_2.

Moreover, Fig. 5.14a shows that for $0 < t < 3.5\,\mathrm{s}$ (mode 1: closed switch, b = 1) the bounds are much wider than for $t > 3.5\,\mathrm{s}$ (mode 0: open switch, b = 0). This would be expected because in (5.37a)–(5.37b) $b = 0$ and f_{C_1} as well as $\dot{f}$ are very small for $t > 3.5\,\mathrm{s}$ (cf. Fig. 5.13b for the time history of the currents $f = i_{R_1}$ and $f_{C1} = i_{C_1}$).

5.3.3 Measurement Uncertainties

Inputs into an incremental bond graph are relative parameter variations $\Delta\Theta_i/\Theta_i$ multiplied by a power variable from the diagnostic bond graph with nominal parameters. If inputs into the diagnostic bond graph obtained either by measurements from the real system or from a behavioural model replacing the real system carry measurement uncertainties then this affects power variables in the diagnostic bond graph that control modulated sinks of the incremental bond graph. As a result, measurement uncertainties have an impact on the variations of ARR residuals and thus on their thresholds.

Figure 5.15 illustrates this situation assuming that measurement uncertainties are additive. A flow $\tilde{f} = \tilde{f}' + \Delta\tilde{f}'$ with a predicted part $\tilde{f}'$ and an uncertain part $\Delta\tilde{f}'$ due to measurement uncertainty is the output of a non-ideal sensor and an input into the diagnostic bond graph. The input $\tilde{f}$ into the diagnostic bond graph results in an effort $e = e' + \Delta e'$ that controls a modulated sink MSe where e' denotes the predicted part and $\Delta e'$ the uncertain part. The output $w_\Theta := \delta(e' + \Delta e')\Delta\Theta$ of the modulated sink is an input into the incremental bond graph that is needed to compute the variation Δr of an ARR residual r.

If measurement uncertainties can be assumed to be bounded, then application of the triangle inequality may yield thresholds for parameter variations of ARR residuals that are independent of measurement uncertainties. For instance, let z' be the predicted part of an output variable z of the diagnostic bond graph that controls a modulated sink of the incremental bond and let $|\Delta z'| \leq b_z$ be the bounded measurement uncertainty. Furthermore, let Δr be the variation of an ARR residual r that depends on z and its derivative. Then

$$\begin{aligned} |\Delta r| &\leq |n_1\,(z' + \Delta z')| + |n_2\,\frac{d}{dt}(z' + \Delta z')| \\ &\leq \underbrace{|n_1\,z'| + |n_2\frac{d}{dt}z'|}_{\leq thr(t)} + |n_1\,b_z| + |n_2\frac{d}{dt}\Delta z'| \end{aligned} \tag{5.39}$$

where n_1 and n_2 are constants.

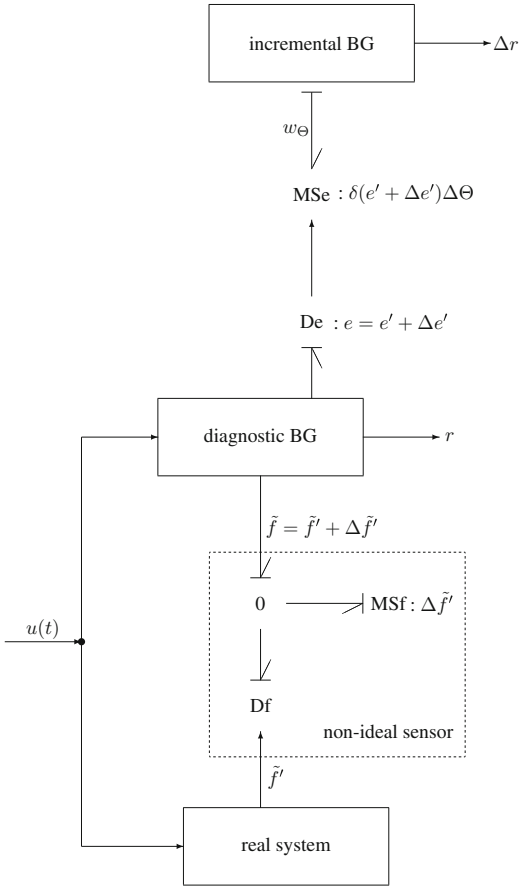

Fig. 5.15 Accounting for measurement uncertainties

If the derivative $\frac{d}{dt}\Delta z'$ is approximated by the difference quotient then

$$|n_2 \frac{d}{dt}\Delta z'| \leq |n_2 \frac{2b_z}{\Delta t}| \tag{5.40}$$

where Δt denotes the sampling time of the measurement.

The result is a threshold $thr'(t) \geq thr(t)$ that is independent of measurement uncertainties but that depends on the sampling rate of the measurement. In [14], Touati et al. have accounted for measurement uncertainties by adding modulated sources to an uncertain bond graph.

The simple model of a non-ideal sensor in Fig. 5.15 accounts for measurement uncertainties by means of a modulated sink. However, a sensor may deliver wrong readings because it operates in a faulty mode due to external disturbances that are caused by changes in the ambient or by internal disturbances such as parametric faults. That is, the computation of ARR residuals and of adaptive thresholds for their

parameter variations may give misleading results. If the build-up and the parameters of a sensor are known, parametric faults as well as a sensor's sensitivity with regard to known external disturbances can be taken into account by a more elaborate bond graph model replacing a simple model such as the one in Fig. 5.15. If, however, details of its internal build-up are not known, then the sensor's dynamic behaviour may be approximately captured for small deviations from its operating point by a transfer function with parameters that at least account for the sensor's time delay and its gain.

5.3.4 Uncertain Excitations

Constant excitations to a system are represented by an effort or a flow source that provides an output of constant value. In the incremental bond graph these sources are replaced by sources of value zero. If a constant excitation, however, is to be considered uncertain, its source may be replaced in the incremental bond graph by a source modulated by the nominal value. For instance, let Se : E_n represent a constant voltage or constant hydraulic pressure supply. If there is a relative uncertainty $\delta_E = \Delta E / E_n$, then the constant effort source may be replaced in the incremental bond graph by an effort source MSe : $\delta_E E_n$ modulated by the nominal effort E_n obtained from the bond graph with nominal parameters. If the internal structure and the parameters of the device are known that provides the excitation and if possible disturbances acting on the device can be modelled, then an incremental bond graph model can be constructed that accounts for the uncertainty of the excitation.

5.4 Summary

ARR residuals as fault indicators should be distinctly sensible to true faults and robust with regard to parameter uncertainties. That is, if parameters varies, the time evolution of ARR residuals should be within prescribed bounds. For real systems described by a hybrid model bounds should be adapted to system modes as the dynamic behaviour can be quite different in different system modes.

This chapter briefly recalls the basic idea of incremental bond graphs and extends their application to switched LTI systems. Incremental bond graphs can be systematically constructed from an original bond graph and retains its structure. They differ from an original bond graph of a hybrid model only by additional sinks. These sinks are introduced by the replacement of bond graph elements with varying parameters by their incremental element model. The additional sinks represent parameter variations and are modulated by a power variable from the original bond graph.

In contrast to an original bond graph, the bonds of an incremental bond graph carry variations of power variables. Outputs of interest with regard to FDI are variations of ARR residuals. For a switched LTI system, these variations are a weighted sum of the

inputs and their derivatives into the incremental bond graph. The weighting factors are the parameter sensitivities of an ARR residual. Model equations and ARRs can be derived in the same manner from an incremental bond graph as from an original bond graph. That is, variations of ARR residuals due to parameter variations and parameter sensitivities of ARR residuals can be derived from an incremental bond graph, while the nominal part of an ARR is obtained from a diagnostic bond graph with nominal parameters. Once the time evolution of parameter sensitivities of ARRs is known, their assessment may give rise to simplify a structural FSM by setting some entries to zero. For switched LTI systems, the principle of superposition may be applied. That is, if only some parameter sensitivities are of interest, only their corresponding bond graph elements may be replaced by their incremental model and increments of ARR residuals be derived from the incremental bond graph.

Furthermore, the expression of variations of ARR residuals as a weighted sum of inputs and their derivatives suggests in a natural way to apply the triangle inequality to obtain adaptive mode-dependent thresholds for variations of ARRs due to parameter variations. That is, parameters may vary. As long as ARR residuals are within these bounds, no fault is reported.

References

1. Borutzky, W. (2009). Bond graph model-based fault detection using residual sinks. *Proc of the Institution of Mechanical Engineers Part I Journal of Systems and Control Engineering.*, *223*(3), 337–352.
2. Samantaray, A. K., & Ghoshal, S. K. (2007). Sensitivity bond graph approach to multiple fault isolation through parameter estimation. *Proceedings of the Institution of Mechanical Engineers Part I: Journal of Systems and Control Engineering*, *221*(4), 577–587.
3. Gawthrop, P. J. (2000). Sensitivity bond graphs. *Journal of the Franklin Institute*, *337*, 907–922.
4. Cabanellas, J. M., Félez J., & Vera C. (1995) A formulation of the sensitivity analysis for dynamic systems optimization based on pseudo bond graphs. In: Cellier F. E., & Granda J. J., (Eds.), *ICBGM'95, International Conference on Bond Graph Modeling and Simulation*. Vol. 27(1) of Simulation Series. Las Vegas, Nevada: SCS Publishing. (pp. 135–144).
5. Borutzky, W., & Granda, J. J. (2002). Bond graph based frequency domain sensitivity analysis of multidisciplinary systems. *Proc Instn Mech Engrs, Part I, Journal of Systems and Control Engineering*, *216*(1), 85–99.
6. Borutzky W., & Granda J. J. (2001) Determining sensitivities from an incremental true bond graph. In: J. J. Granda & G. Dauphin-Tanguy (Eds.), *2001 International Conference on Bond Graph Modeling, and Simulation (ICBGM 2001)*. Vol. 33(1) of Simulation Series. Phoenix, Arizona: SCS Publishing (pp. 3–8).
7. Borutzky, W. (Ed.). (2011). *Bond Graph modelling of engineering systems—theory, applications and software support*. New York: Springer.
8. Merzouki, R., Samantaray, A., Pathak, P., & Ould Bouamama, B. (2013). *Intelligent mechatronic systems*. Berlin: Springer.
9. Djeziri, M. A., Merzouki, R., Ould Bouamama, B., & Dauphin-Tanguy, G. (2007). Robust fault diagnosis by using bond graph approach. *IEEE/ASME Transactions on Mechatronics*, *12*(6), 599–611.
10. Djeziri, M. A. (2007) Diagnostic des sysèmes incretains par l'Approche bond graph [PhD thesis]. Ecolde Centrale de Lille, France. Available from: http://hal.archives-ouvertes.fr/docs/00/20/00/30/PDF/These-Djeziri-07-12-2007.pdf.

11. CadSim Engineering. CAMPG, Available from: http://www.bondgraph.com.
12. The Mathworks: MATLAB—the language of technical computing. Available from: http://www.mathworks.com/products/matlab/.
13. Scilab Enterprises: Scilab. 78000 Versailles, France. Available from: http://www.scilab.org/.
14. Touati, Y., Merzouki, R., & Ould Bouamama, B. (2011) Fault detection and isolation in presence of input and output uncertainties using bond graph approach. In: A. Bruzzone & G. Dauphin-Tanguy, S. Junco, M. A. Piera (Eds.) *Proceedings of the 5th International Conference on Integrated Modeling and Analysis in Applied Control and Automation (IMAACA 2011)*. DIPTEM University of Genoa (pp. 221–227).